CrossMark

Strong coupling of centennial-scale changes of Asian monsoon and soil processes derived from stalagmite $\delta^{18}O$ and $\delta^{13}C$ records, southern China

Dianbing Liu [a], Yongjin Wang [a,*], Hai Cheng [b,c], R. Lawrence Edwards [b], Xinggong Kong [a], Ting-Yong Li [d]

[a] College of Geography Science, Nanjing Normal University, Nanjing 210023, China
[b] Department of Geology and Geophysics, University of Minnesota, Minneapolis, MN 55455, USA
[c] Institute of Global Environmental Change, Xi'an Jiaotong University, Xi'an 710049, China
[d] School of Geographical Sciences, Southwest University, Chongqing 400715, China

ARTICLE INFO

ABSTRACT

The paleoclimate application of speleothem $\delta^{13}C$ is influenced by site-specific processes. Here we present four stalagmite $\delta^{13}C$ records from two caves in southern China, covering early and late Marine Isotope Stage (MIS) 3 and the Holocene, to investigate the spatio-temporal pattern of calcite $\delta^{13}C$ changes and the relationship with Asian monsoon (AM) variability. In each growth period, precessional- to millennial-scale changes are clear in the $\delta^{18}O$ record. In contrast, millennial variability is absent in the $\delta^{13}C$ record, which characterizes persistent centennial oscillations. However, centennial-scale $\delta^{18}O$ variations agree well with those of $\delta^{13}C$, with a larger amplitude in $\delta^{13}C$ changes (about twice that of $\delta^{18}O$). This suggests that soil humidity balance associated with regional hydrological circulations is important for these centennial $\delta^{13}C$ changes, although evaporation-related kinetic fractionation can induce concurrent enrichments in $\delta^{18}O$ and $\delta^{13}C$. In frequency, the detrended $\delta^{18}O$ and $\delta^{13}C$ records are coupled at a periodicity of about 300 yr during the last glacial period and 150 yr during the Holocene. Those centennial-scale $\delta^{13}C$ variations are generally consistent with Greenland temperature variability, indicating a climate response over broad regions. Thus, strong co-variation of $\delta^{18}O$ and $\delta^{13}C$ records should have a climatic origin, even if it is amplified by kinetic effects.

© 2016 University of Washington. Published by Elsevier Inc. All rights reserved.

Introduction

The use of speleothem $\delta^{13}C$ in paleoclimate studies is hindered by the complexity of carbon transfer/exchange between gas−liquid−solid phases of calcite dissolution and precipitation (McDermott, 2004; Fairchild et al., 2006), which is associated with climatically related and site-specific processes. In western Europe, multiple-cave studies showed that about 60−90% of carbon in stalagmites sources from soil CO_2 by plant respiration and microbiological decomposition (Genty et al., 2001, 2003). These cave sites are geographically widespread within a latitudinal band of 40−55°N and covered by different vegetation types. The annual mean temperature ranges from 7.3°C to 14.5°C. In a theoretical study, the biological CO_2 contribution of 50−60% was also proposed by Hendy (1971), depending on cave system (i.e., whether the infiltrating water dissolving the carbonate is permanently in contact with soil CO_2 or remains isolated from a gas phase until its emergence in the cave). This biogenic $\delta^{13}C$ signal contained in the infiltration water is further modulated by cave temperature and dripping rates (Mühlinghaus et al., 2007, 2009; Johnston et al., 2013), in-cave ventilation and evaporation conditions (Scholz et al., 2009; Johnston et al., 2013; Dreybrodt and Deininger, 2014), and prior calcite precipitation (Baker et al., 1997). These processes probably cause isotopically kinetic fractionation at the solid−solution interface when stalagmite precipitates, and thus deviate the carbon isotopic ratio from the primary climate signal.

However, the complex behavior of carbon isotopes reported in these monitoring and laboratory studies often operates at the seasonal scale or less. On millennial to centennial scales, multi-

proxy studies (that include stalagmites) are instrumental to understand the correlation of climate and calcite $\delta^{13}C$ variability, if the $\delta^{13}C$ signal is closely related to soil CO_2 changes.

At climatically and environmentally sensitive sites, speleothem $\delta^{13}C$ records have been successfully applied to track orbital- to multi-decadal climate variability and soil CO_2 production (Burns et al., 2002; Genty et al., 2003; Cruz et al., 2006). In some cases, the calcite $\delta^{13}C$ signal was suggested to be more sensitive to climate changes than the $\delta^{18}O$ record (Frappier et al., 2002; Genty et al., 2003; Hodge et al., 2008; Scholz et al., 2012), and the seasonal to annual $\delta^{13}C$ cycles have been used as a chronological tool to constrain the time scale of non-laminated stalagmites (Meyer et al., 2014; Ridley et al., 2015). Nevertheless, a positive relationship between stalagmite $\delta^{18}O$ and $\delta^{13}C$ values along the growth axis, i.e. influenced by evaporation and ventilation effects, was cautioned to be an indication of kinetically fractionated deposition (Hendy, 1971), and such speleothems can not be used to give paleoclimate data. Mickler et al. (2006) compiled 165 widely-separated speleothem $\delta^{18}O$ records and found that kinetic isotope effect is a prevalent phenomenon. It appears that the primary climate signal in stalagmites should not be swamped by these kinetic effects, especially at millennial to centennial scales. Furthermore, recent modeling and theoretical studies also suggested that in a cave of high humidity (greater than 85%) and poor ventilation (smaller than 0.2 m/s), which represents the typical cave environments in the field, evaporation effect does not change the isotopic composition of precipitated calcite in the same direction (Deininger et al., 2012; Dreybrodt and Deininger, 2014). Hence, co-variation of $\delta^{13}C$ and $\delta^{18}O$ might not exclude their applicability in paleoclimate reconstructions (Mickler et al., 2006; Romanov et al., 2008; Dorale and Liu, 2009).

In eastern China, speleothem $\delta^{13}C$ (local effective moisture) from Hulu Cave exhibited a complicated correlation with $\delta^{18}O$ records (Asian monsoon [AM] variability) in the last glacial (positive at orbital scale but negative at millennial scale) (Kong et al., 2005). At the onset of Dansgaard-Oeschger (DO) events, the AM rise was synchronous with increase of effective moisture, but at the end of DO events the AM decline significantly lagged changes of local humidity. Different dynamics were thus invoked to explain the $\delta^{13}C$ behavior, specifically changes of C_3/C_4 vegetation type at the orbital scale and dissolution of biogenic CO_2 associated with the dilution effect of infiltration water at the millennial scale. However, in the last deglacial, a positive relationship between decadal changes of $\delta^{18}O$ and $\delta^{13}C$ suggests that the spatio-temporal significance of $\delta^{13}C$ records at the Hulu site left open a substantial window of interpretation. At orbital to millennial scales, speleothem $\delta^{18}O$ records from the AM area have been proven to be well correlated (Cheng et al., 2012), but significant disparity arises at centennial scale, such as a gradual or abrupt onset of DO12 (Burns et al., 2003; Cai et al., 2006). At the Hulu site, DO15 and 9 in the $\delta^{18}O$ record (lasting about 100–200 yr) are well correlated with enrichments in $\delta^{13}C$ values, implying a potential role of calcite $\delta^{13}C$ in understanding centennial climate changes.

Motivated by this idea, we further present spatially separated speleothem records to investigate the dynamics of $\delta^{13}C$ variability under different climate backgrounds. In previous studies, three- to seven-yr resolution AM changes have been reported during the Holocene (Wang et al., 2005; Duan et al., 2014a) and early Marine Isotope Stage (MIS) 3 (Liu et al., 2010) from stalagmite-based $\delta^{18}O$ records from Dongge and Wulu caves in southern China. Here we first present the carbon isotope archives from these records, together with a newly retrieved late MIS 3 stalagmite (Wu66) $\delta^{13}C$ record from Wulu Cave, allowing an evaluation on multi-decadal to centennial-scale $\delta^{13}C$ variability under different climate conditions.

Sites, samples and methods

Wulu and Dongge caves are located at the Yun-Gui Plateau, southern China (Supplementary Fig. 1), and the exposed carbonate rock areas at these sites are strongly influenced by rocky desertification. Wulu Cave (26°03′N, 105°05′E, 1440 m above sea level) is in the southwest of Guizhou Province, while Dongge Cave (25°17′N, 108°5′E, with an elevation of 680 m) is located 300 km to the southeast. The hill at the Wulu site has a slope of over 60°, and about 40°−50° at Dongge Cave. The regional climate conditions are influenced by the subtropical East Asian and tropical Indian summer monsoons. Local precipitation distinctly increases in late spring as the Indian monsoon intensifies. In summer, the meteorological conditions are dictated by both the Indian and East Asian summer monsoons.

Modern vegetation at the Wulu site is mostly composed of deciduous herbs (C_4-type vegetation). The cave is about 800 m long, overlain by 40 m of Triassic limestone bedrock. A thin patchy soil cover (5−10 cm) above the cave is only observed in the fractures and karstic depressions. The inner part of the cave chamber (500−800 m from the entrance) is covered by 2-m-high deposits of clay and debris. It is poorly ventilated in this chamber, and the temperature inside approximates the annually averaged surface temperature with a relative humidity of about 100%. Mean annual temperature at this site is about 14°C, with a maximum in July (20.8°C) and a minimum in January (4.3°C). The annual precipitation is about 1400 mm, peaking (900 mm) during the summer (June through September), reaching a minimum (80 mm) in the winter (December to February).

Densely forested vegetation at the Dongge Cave consists primarily of evergreen broad-leaved plants. In this area, the limestone soil (20−40 cm thick) is discontinuously distributed. In the soil profile, AF horizon is immediately above the parent rock, with a thickness of less than 10 cm. The cave is about 1110 m long, beneath over 100 m of Carboniferous limestone. The relative humidity inside is close to 100%. Current air temperature at this site is 15.6°C, reaching a maximum in July (27°C) and a minimum in January (5.5°C). Mean annual precipitation near Dongge Cave is 1750 mm. Most of the rainfall (80%) occurs between May and October when monsoonal convective rainfall prevails, with much less precipitation (20%) occurring between November and April.

Rocky desertification in southwestern China was first reported in AD 1638, and described as "rocky landscape almost devoid of soil and vegetation" in "Xu Xiake's Travels". It is believed to pervasively appear around 4 ka with a strong disturbance from human activities (Jiang et al., 2014). Pollen records near Dongge Cave suggested that woody plants occurred between 5.5 and 4.5 ka in this area, and then grass species increased with a decline in regional temperature and precipitation (Du et al., 2013). Around the Wulu site, sparse herbs and ferns were major components of the local ecosystem between 45 and 42.5 ka when the climate was cold, followed by a vegetation type of trees and shrubs from 42.5 to 41.3 ka (Zhao et al., 2012). This implies that in the distant warm and humid periods, woody vegetation should have occurred at the Wulu site.

Two stalagmites (DA and DAS) were collected from Dongge Cave. Sample DA is 963 mm high, with a diameter of 170−200 mm (Wang et al., 2005). When halved and polished, it is composed of transparent and milky calcite, lacking obvious growth interruptions. Stalagmite DAS is 590 mm long, and has a 'candlestick' shape with a diameter of 120 mm (Duan et al., 2014a), indicating a stable deposition history. Its lithological character is similar to Sample DA.

Samples Wu23 and Wu66 were collected in the inner chamber of Wulu Cave. Stalagmite Wu23 is 667 mm in length (Liu et al.,

2010). It has a 'candlestick' shape and a diameter of ~65 mm. The newly retrieved sample Wu66 is 581 mm long with a diameter of 60 mm. Clay bands and/or shifts of the stalagmite apex can be observed at 22, 100, 165 and 355 mm (gray bars in Fig. 1a), probably indicating changes in the ventilation patterns, inclusion content, degassing rate or even growth discontinuities.

Five calcite powder sub-samples were collected along the growth axis of sample Wu66 with 0.9-mm-diameter carbide dental burrs for ^{230}Th dating. The measurements were performed by inductively coupled plasma mass spectrometry (ICP-MS) on a Finnigan-MAT Element at the Department of Geology and Geophysics, University of Minnesota, USA. The chemical procedures used to separate uranium and thorium are similar to those described in Shen et al. (2002). Dating results are listed in Table 1, with typical analytical errors (2σ) ranging from 150 to 240 yr.

For stable isotopic measurements, 576 sub-samples were drilled on sample Wu66 with 0.3-mm-diameter carbide dental burrs. Analyses were performed on a Finnigan-MAT 253 mass spectrometer fitted with a Kiel Carbonate Device at the College of Geography Science, Nanjing Normal University. Spatial resolution is 1 mm, equivalent to an average temporal resolution of 5 yr. The results are reported relative to Vienna PeeDee Belemnite (VPDB) with standardization determined relative to NBS 19. Precision of δ^{18}O values is 0.06‰ and 0.03‰ for δ^{13}C, at the 1-sigma level.
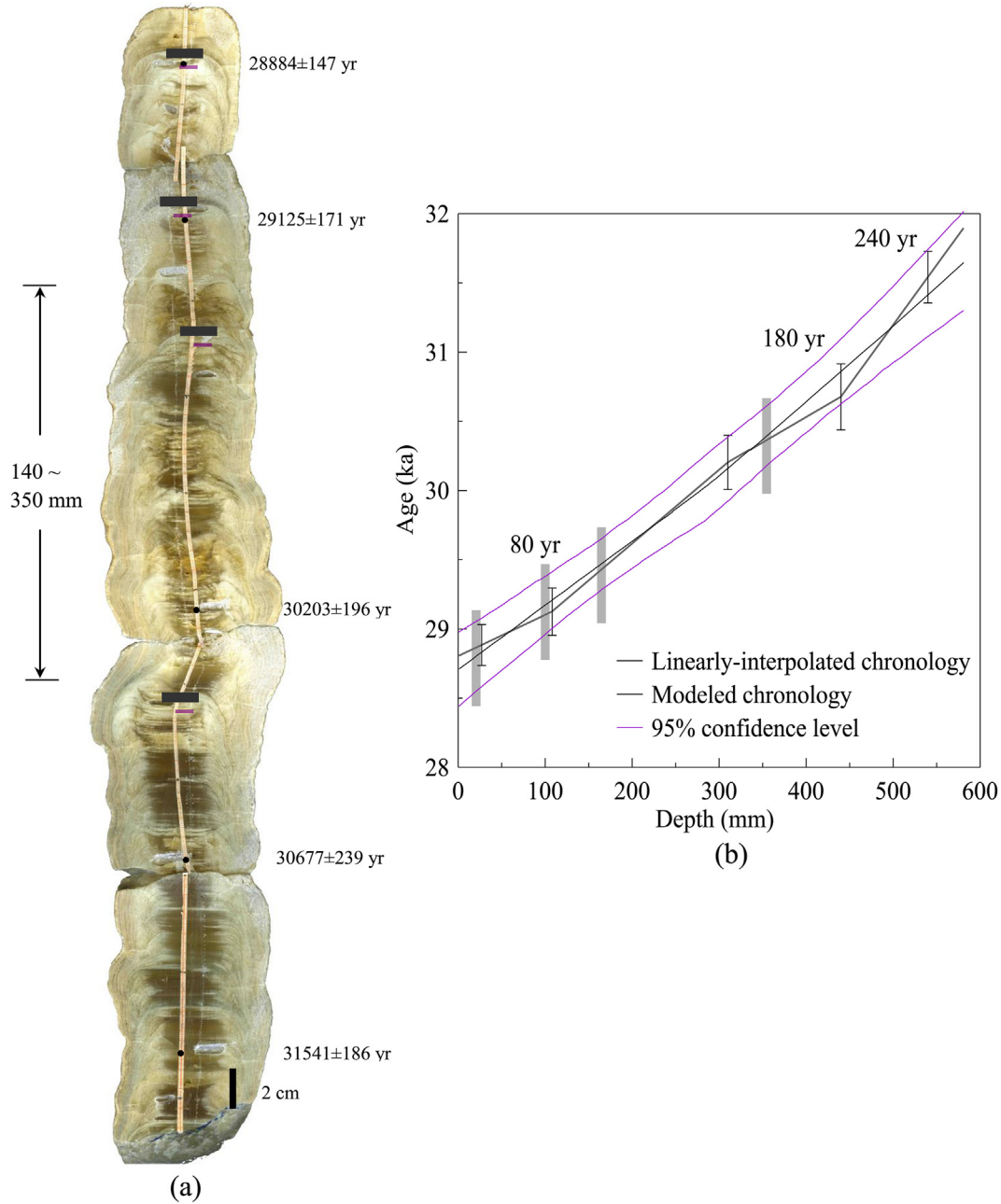

Figure 1. Polished section (a) and the age model (b) of stalagmite Wu66. The black dots and gray bars in profile (a) represent the positions of U/Th dates and lithological anomalies, respectively. The transition from DO4.1 to H3 (between 350 mm and 140 mm) is indicated on the left. In panel b, the black and purple lines show the age model by the algorithm method of MOD-AGE (Hercman and Pawlak, 2012) and the 95% confidence level. The gray line and the gray bars show the linearly interpolated ages and depths of lithological anomalies. Temporal offsets between the modeled and linearly interpolated ages are indicated by the numbers. (For interpretation of the references to color in this figure legend, the reader is referred to the web version of this article.)

Table 1
[230]Th dating results for sample Wu66 from Wulu Cave, southern China.

Sample number	Depth (mm)	[238]U (ppb)	[232]Th (ppt)	δ^{234}U (measured)	[230]Th/[238]U (activity)	[230]Th age (yr) (uncorrected)	[230]**Th age (yr) (corrected)**	δ^{234}U$_{Initial}$ (corrected)
Wu66-27	27	10,939.2 ± 40.8	1060 ± 22	709.6 ± 3.5	0.405 ± 0.002	28,948 ± 147	**28,884 ± 147**	770 ± 4
Wu66-108	108	13,341.2 ± 58.7	528 ± 11	712.4 ± 3.8	0.409 ± 0.002	29,187 ± 171	**29,125 ± 171**	774 ± 4
Wu66-310	310	16,083.5 ± 78.2	387 ± 8	697.6 ± 4.0	0.419 ± 0.002	30,266 ± 196	**30,203 ± 196**	760 ± 4
Wu66-440	440	16,556.8 ± 98.4	227 ± 5	709.2 ± 4.8	0.427 ± 0.003	30,739 ± 239	**30,677 ± 239**	773 ± 5
Wu66-540	540	12,778.5 ± 56.2	184 ± 4	691.0 ± 3.8	0.433 ± 0.002	31,603 ± 186	**31,541 ± 186**	756 ± 4

Errors are 2σ analytical errors. Decay constant values are $\lambda_{230} = 9.1577 \times 10^{-6}$ yr^{-1}, $\lambda_{234} = 2.8263 \times 10^{-6}$ yr^{-1}, $\lambda_{238} = 1.55125 \times 10^{-10}$ yr^{-1}. Corrected [230]Th ages assume an initial [230]Th/[232]Th atomic ratio of $(4.4 \pm 2.2) \times 10^{-6}$. Corrected [230]Th ages are indicated in bold, and presented in years before AD 1950.

Results

Five [230]Th dates, with high uranium (~10–17 ppm) and low thorium concentrations (generally less than 600 ppt) (Table 1), reveal that sample Wu66 grew during late MIS 3 (31.5–28.9 ka). All ages were corrected for initial [230]Th using the value $(4.4 \pm 2.2) \times 10^{-6}$, a value calculated from the initial [230]Th/[232]Th ratio, and these corrections introduced inconsequential changes to

the resulting ages. An age model of the stable isotopic data was developed by an algorithm approach, MOD-AGE (Hercman and Pawlak, 2012), which used the locally weighted scatterplot smoothing method (Fig. 1b). The modeled chronology agrees well, within 95% confidence level, with the linearly interpolated age.

Temporally, sample Wu66 covered a period from DO 4.1 to Heinrich (H) event 3 (31–29 ka). The DO 4.1 in Wu66 (gray bar in Fig. 2b) is synchronous with Wu3 record from the same cave
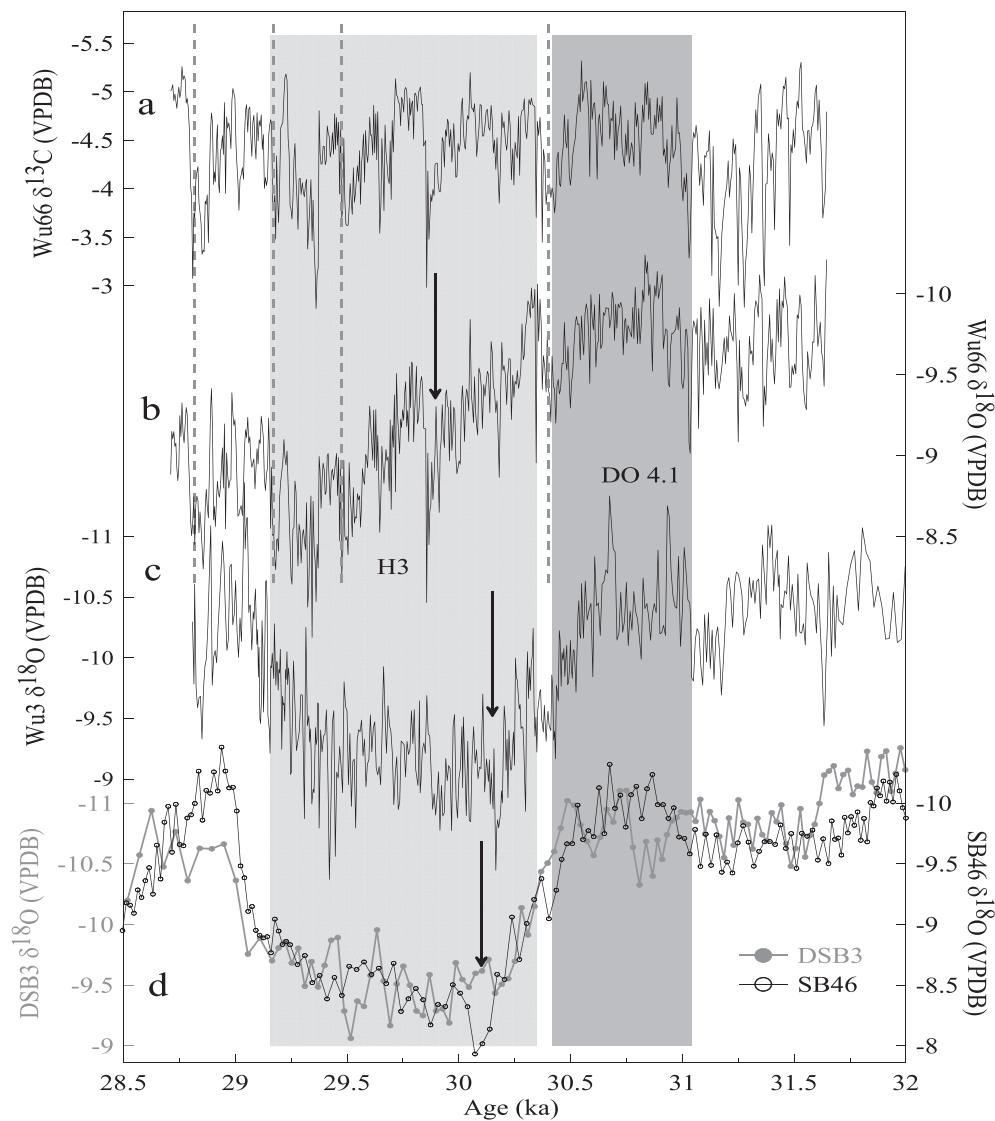

Figure 2. Regional correlation of the cave records surrounding DO4.1 event. From the upper to bottom are Wu66 δ^{18}O and δ^{13}C (a, b; this study) and Wu3 δ^{18}O records (c; Duan et al., 2014b) from Wulu Cave, δ^{18}O records from Dashibao Cave, southern China, and Sanbao Cave, central China (d; Zhao et al., 2010). The DO4.1 is constrained by the gray bar, the H3 event is expressed by the crossed bar. The dotted lines indicate the positions of lithological changes in sample Wu66. The arrowed lines show the sharp decline of AM intensity at the end of DO4.1/H3 transition.

(Fig. 2c) (Duan et al., 2014b) and other cave records from central and southern China (Fig. 2d) (Zhao et al., 2010). This partly supports the reliability of our modeled chronology. A significant discrepancy between them can be observed between 30.5 and 29.4 ka, during which Wu66 δ^{18}O record characterizes a more gradual positive excursion (crossed bar in Fig. 2b). Noteworthy in these cave records is an abrupt increase in δ^{18}O values at the end of the DO4.1/H3 transition (arrowed lines in Fig. 2b–d), the timing of which appears 200 yr younger in Wu66 record. An explanation of larger residence time of seepage water at the Wulu site is apparently inconsistent with the observed synchroneity of DO 4.1 between them. We note that lithological changes are evident at 100 mm (~29.2 ka), 165 mm (~29.5 ka) and 355 mm (~30.4 ka) in Wu66, separately distributing over the gradual positive δ^{18}O excursion (gray dotted lines in Fig. 2a and b). It is likely that short-lived growth cessations potentially occurred at these depths, which is unrecognized by U/Th ages due to their 200-yr dating errors (Table 1) and the modeled age as the growth hiatus in this model is often treated as a slowdown of the deposition rate rather than total stagnation (Hercman and Pawlak, 2012). Despite this discrepancy, the general agreement of these δ^{18}O records implicates a climatic origin, linked to rainfall isotopic composition associated with changes of the AM intensity (Wang et al., 2005).

During the growth period, three stages are clear in Wu66 δ^{18}O record: a plateau in δ^{18}O values (with a mean value of −9.8‰) prior to 30.5 ka, a long-term enrichment (from −10 to −8‰) between 30.5 and 29.4 ka, and a subsequent depletion in δ^{18}O values (Fig. 2b). In contrast, the δ^{13}C record characterizes persistent multi-decadal to centennial-scale oscillations between −5‰ and −3.5‰ (Fig. 2a). The DO 4.1 and a series of decadal δ^{18}O enrichments are well-reflected in the δ^{13}C record, implicating a tight correlation between them. Before 30.5 ka, however, the decadal δ^{13}C oscillations exhibit larger amplitude than the δ^{18}O.

When compared with the previous speleothem records, orbital-to millennial-scale changes are evident in the δ^{18}O records in early (Fig. 3d) (Liu et al., 2010) and late MIS 3 (Fig. 3c) and the Holocene (Fig. 3a and b) (Wang et al., 2005; Duan et al., 2014a). Superimposed on the orbital to millennial variability, minor δ^{18}O enrichments (0.5–1‰) at multi-decadal to centennial scales can be observed. In contrast, changes of the δ^{13}C show a strikingly different pattern. First, orbital- to millennial-scale variability is absent in the δ^{13}C records. To some degree, the δ^{13}C variations are confined to their fixed background values (horizontal gray lines in Fig. 3), i.e. fluctuating around their mean values (−5.4 to −5.6‰ during the Holocene, −8.1‰ and −4.4‰ in early and late MIS 3). Second, centennial-scale δ^{13}C oscillations are exceptionally clear and persist throughout each growth period. Changes of δ^{13}C values generally fall within their envelopes of one standard deviation and are generally larger than 0.8‰ in amplitude (dotted gray lines in Fig. 3). Third, high-frequency (multi-decadal to centennial) δ^{18}O changes are closely correlated to the δ^{13}C signals, regardless of their divergence at the low-frequency domain. When detrended, centennial-scale enrichments of the residual δ^{18}O (δ^{18}O$_d$) are well mirrored in the δ^{13}C (Supplementary Fig. 2).

It has been proposed that changes in stalagmite growth rate exert an appreciable impact on the stable isotope composition (Kong et al., 2005; Dreybrodt and Scholz, 2011; Feng et al., 2014; Stoll et al., 2015), with an enhancement in growth rate corresponding to more negative isotopic values (Dreybrodt and Scholz, 2011; Stoll et al., 2015) and/or larger amplitude of centennial-scale variations (Kong et al., 2005). When compared with the U/Th-based growth rate records (Supplementary Fig. 3), a weak correlation can be observed between the growth rate and isotopic records. Furthermore, changes of detrended δ^{13}C/δ^{18}O in each time period are generally within a range of 0 and 2, independent of shifts

in calcite deposition. These lines of evidence, combined with the agreement of spatially separated δ^{18}O records (Fig. 2), indicate that these stalagmites likely precipitated close to isotopic equilibrium conditions (Dorale and Liu, 2009).

Discussion

Duplication test of speleothem δ^{13}C records

In each time window we evaluated, changes of the calcite δ^{13}C at these sites exhibit a similar pattern over contemporaneous periods (Fig. 4). These δ^{13}C records show persistent multi-decadal to centennial oscillations around their constant mean values. At a centennial scale, shifts of the δ^{13}C values are generally within an amplitude of 1–1.5‰.

In early MIS 3 (Fig. 4a), a growth discontinuity occurred between 59.3 and 57.7 ka in sample Wu26. A close agreement of Wu26 and Wu23 δ^{13}C records can be observed prior to 59.3 ka. After 57.7 ka, the amplitude of Wu23 δ^{13}C changes appears larger than stalagmite Wu26. However, the agreement of sub-millennial changes in Wu26 and Wu23 δ^{18}O records (Liu et al., 2010) and the regularity of centennial Wu23 δ^{13}C variability (Fig. 4a) suggests that the slight discrepancy between their δ^{13}C records can not be explained by sample-specific processes associated with Wu23 deposition, as its growth rate exhibited little variability during this time (Supplementary Fig. 3d). Other reasons, such as the impact of different degassing rates on calcite δ^{13}C values, should be included (Dreybrodt and Scholz, 2011).

During late MIS 3, centennial-scale Wu66 δ^{13}C shifts are generally consistent with the Wu3 record from the same cave, including the enrichment events around 31.3, 29.8, and 29.3 ka and depletion events at about 31.5, 30.3, and 29.1 ka (Fig. 4b). Regardless of this resemblance, Wu3 δ^{13}C values are systematically more negative. These stalagmites were collected from a 5-m-high cave chamber, with no stalactites hanging over them. Stalagmite Wu3 is about 3 m high with a diameter of 80–120 mm (Duan et al., 2014b), the apex of which is closer to the cave ceiling. This means that the splashing effect of infiltration water feeding stalagmite Wu3 might be weaker in its growth history, possibly resulting in less outgassing of ^{12}C-rich CO_2 (Mühlinghaus et al., 2009) and depleted calcite δ^{13}C values. On the other hand, it could be a primary signal due to different processes happening in the epikarstic, soil, etc.

Among these records, a strong similarity can be identified between DA and DAS δ^{13}C records (Fig. 4c). Both records agree well regarding their absolute values and amplitude of centennial variability. A slight offset between them occurs in a period of 3.7 to 2.3 ka, when DA δ^{13}C values are relatively enriched. Comparatively, the coeval DA δ^{18}O values are more positive than DAS (Supplementary Fig. 4). During this time, the DAS growth rate is indeed larger than sample DA (Supplementary Fig. 3), which potentially results in negative isotopic values in the former (Dreybrodt and Scholz, 2011; Stoll et al., 2015). However, the relationship of synchronous centennial-scale variability between them does not break down in this period.

The difference between δ^{18}O and δ^{13}C changes at orbital to millennial scales (Fig. 3) implies that precessional to millennial AM changes exert little impact on the calcite δ^{13}C signal. As previously suggested, the constant calcite δ^{13}C evolution might reflect the 'vegetation baseline values' (Lambert and Aharon, 2011; Meyer et al., 2014). Hence, the fixed background δ^{13}C values at these sites suggest a stable evolution history of the soil conditions or biological activities. At decadal to centennial scales, however, sample-specific and site-specific discrepancies (Fig. 4) might be explained by different dripping and degassing rates, sampling resolution and/or dating uncertainties. Considering multiple
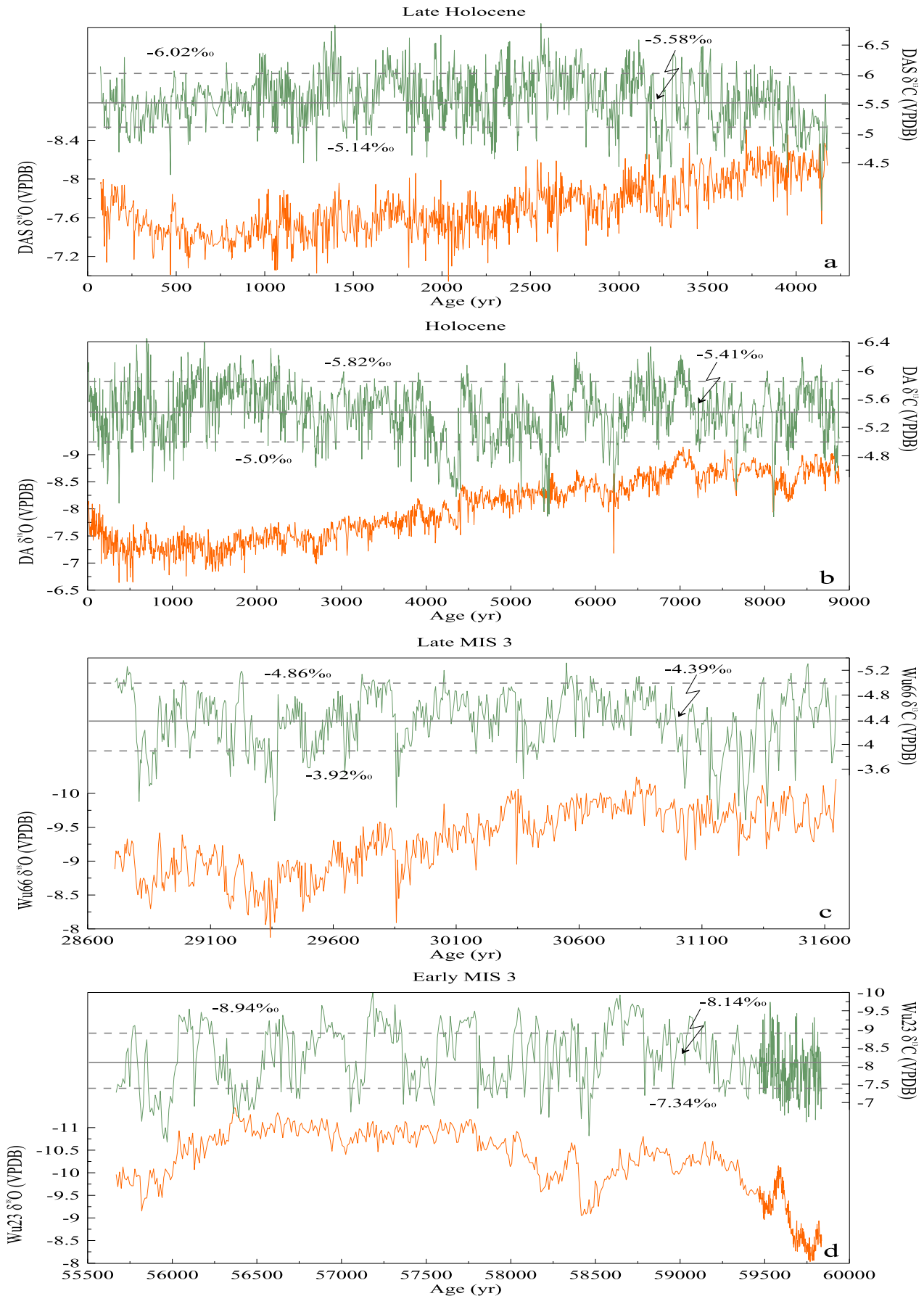
Figure 3. Comparison of speleothem $\delta^{18}O$ and $\delta^{13}C$ records from Dongge and Wulu Caves. (a) Sample DSA ($\delta^{18}O$ from Duan et al. (2014a)), (b) sample DA ($\delta^{18}O$ from Wang et al. (2005)), (c) Wu66 (this study) and (d) Wu23 ($\delta^{18}O$ from Liu et al. (2010)). The gray and dotted gray lines in each panel show the mean values and standard deviations of $\delta^{13}C$ records.
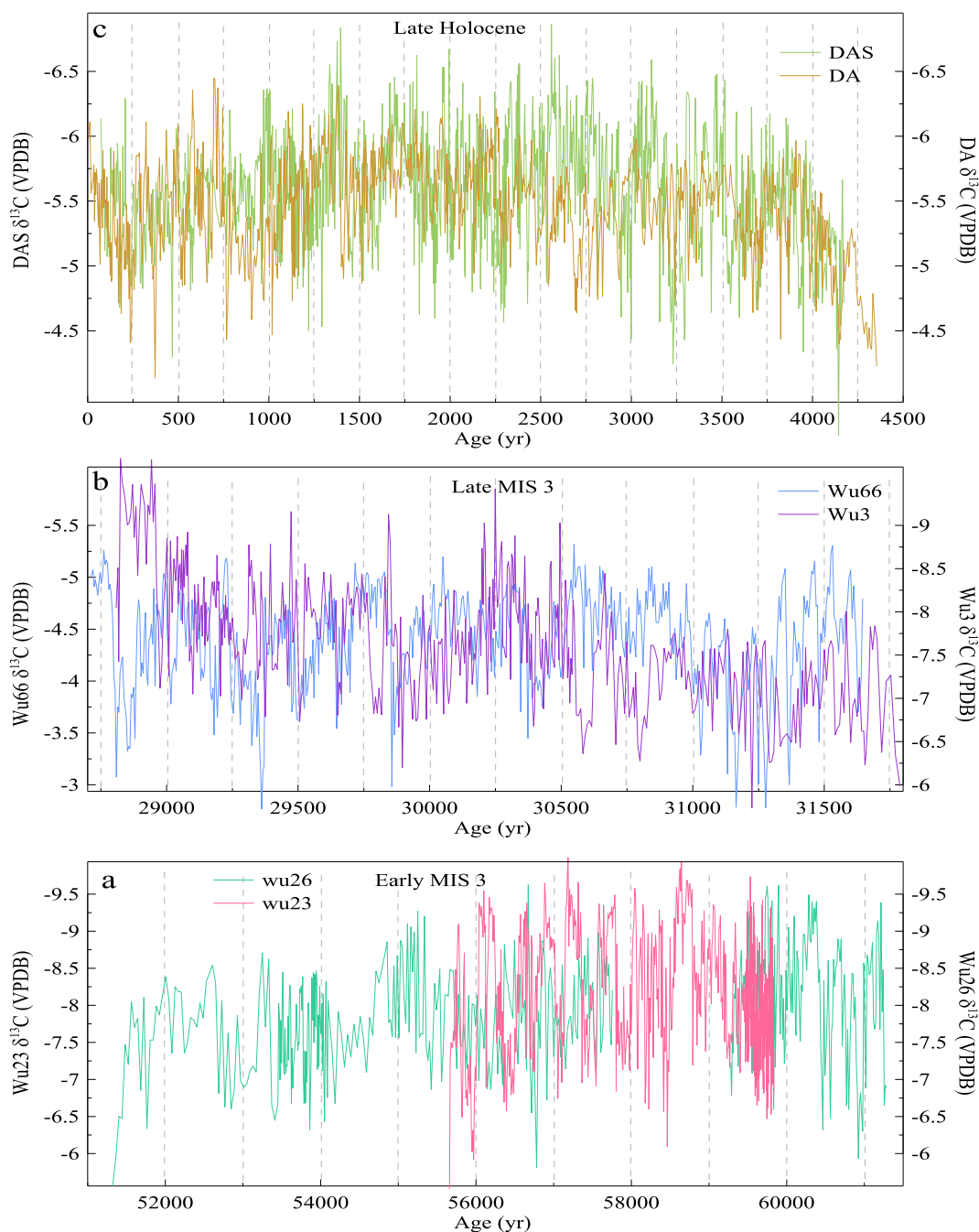
Figure 4. Duplication tests of δ¹³C records. (a) Wu23 and Wu26 δ^{13}C records in early MIS 3, (b) Wu66 and Wu3 δ^{13}C records in late MIS 3, (c) DA and DAS δ^{13}C records in the last 4.2 ka.

controls on the speleothem δ^{13}C signal (McDermott, 2004; Fairchild et al., 2006), the kinetic effect can not be ruled out by our comparison, and it possibly contributes to the offset between samples DA and DAS from 3.7 to 2.3 ka (Supplementary Fig. 4). Despite those dissimilarities, the observed coherence between the δ^{13}C records from the same cave and spatially separated sites (Fig. 4), at least, indicates a common forcing mechanism.

Coupling of centennial changes in the AM and soil processes

Changes of DA and DAS δ^{13}C records have a standard deviation of 0.4‰ (Fig. 3a and b), and 0.5 and 0.9‰ for Wu66 and Wu23,

respectively (Fig. 3c and d). In each centennial cycle, the magnitude of these δ^{13}C changes approximates 0.8–1‰. Shifts of the δ^{13}C at the onset and end of the enrichment periods are very rapid, generally within decades.

To remove any sample-specific noises, the detrended δ^{13}C ($\delta^{13}C_d$) record is applied (Fig. 5). At a centennial scale, changes of the $\delta^{13}C_d$ are closely correlated with the $\delta^{18}O_d$. During the four time windows, a weaker correlation (r = 0.4, n = 640) is observed during early MIS 3 (Fig. 5d), the highest (r = 0.8, n = 575) is in late MIS 3 (Fig. 5c), and over 0.6 in the Holocene (r = 0.6, n = 1177, Fig. 5a; r = 0.7, n = 2116, Fig. 5b). This correspondence is exceptionally pronounced in the weak AM intervals, when increase of $\delta^{18}O_d$

values is obviously coeval with enhancement of the $\delta^{13}C_d$. The durations and amplitudes for the isotopic enrichment/depletion events are comparable. This tight link indicates that centennial-scale changes of both isotopic signals might have the same forcing mechanism and/or the climatic and environmental changes influence them in the same direction.

Typically, the carbon isotopes are incorporated into speleothems as dissolved inorganic carbon (DIC). The dominant DIC species is bicarbonate (HCO_3^-), the initial isotopic signal of which is strongly impacted by soil CO_2, soil-respired CO_2 and degradation of soil organic matter (SOM) (McDermott, 2004; Fairchild et al., 2006). The soil carbon cycling is closely related to changes of temperature
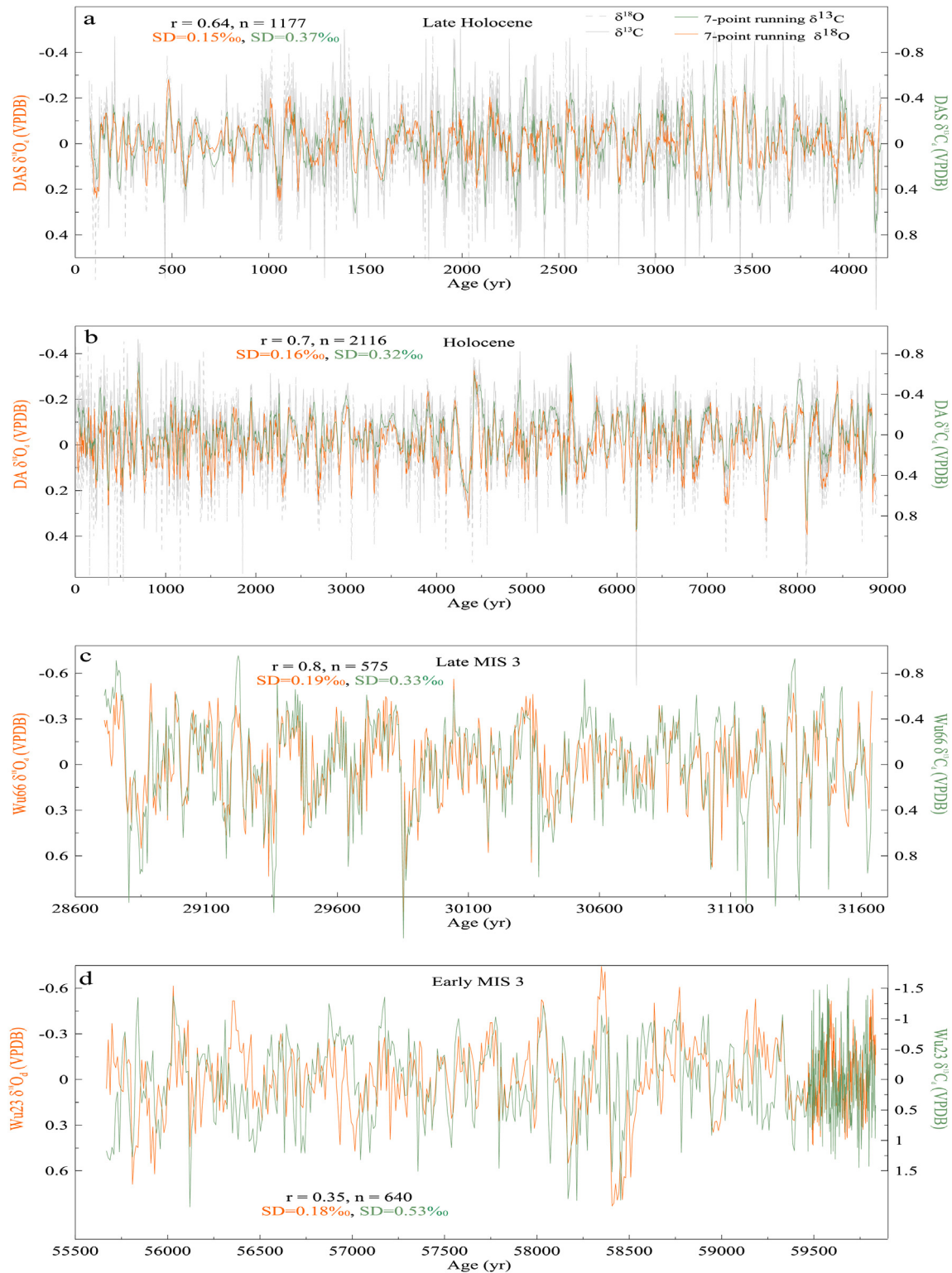

Figure 5. The relationship between detrended $\delta^{18}O$ ($\delta^{18}O_d$) and $\delta^{13}C$ ($\delta^{13}C_d$) records from samples DAS (a), DA (b), Wu66 (c) and Wu23 (d). In each panel, the correlation coefficients between them and the standard deviations for individual records are labeled.

and precipitation (Trumbore, 1997; Conant et al., 2011; Carvalhais et al., 2014), with an overall mean global carbon turnover time of about 20 yr (Trumbore, 1997; Carvalhais et al., 2014). Moreover, the soil temperature and humidity are prominent limiting factors for vegetation growth, soil organic matter decomposition, microorganism activity and root respiration (Kirschbaum, 1995; Trumbore, 1997; Arnone et al., 2008; Grünzweig et al., 2009; Conant et al., 2011). The warming and wetting climate conditions will promote the biological activity, and hence enhance the soil CO_2 production. Generally, the isotopic composition of biogenic soil CO_2 is depleted in ^{13}C (Cerling et al., 1991), with a high soil CO_2 partial pressure (ρCO_2) corresponding to low $\delta^{13}C$ values (Keeling et al., 1979). This isotopic signal can be reflected in the speleothems (Hellstrom et al., 1998; Genty et al., 2003, 2006; Blyth et al., 2013). Thus, the climate-related biogenic CO_2 production associated with plant respiration and microbiological decomposition possibly has a significant impact on the speleothem growth and $\delta^{13}C$ signal (Hellstrom et al., 1998; Genty et al., 2003, 2006). On the other hand, the concurrent enrichments in $\delta^{13}C$ and $\delta^{18}O$ values might indicate an evaporation-related kinetic effect on the isotopic composition during weak AM periods (Mickler et al., 2004; Deininger et al., 2012). However, the kinetic effect can not explain synchronous depletion of $\delta^{13}C$ and $\delta^{18}O$ because the growth rate shows no corresponding variability with the isotopic records (Supplementary Fig. 3).

An inverse correlation of millennial-scale $\delta^{13}C$ and $\delta^{18}O$ changes has been reported at Hulu Cave (Kong et al., 2005). This relationship holds during DO 15, which lasts about 100–200 yr, in stark contrast to the positive correlation of centennial-scale $\delta^{13}C_d$ and $\delta^{18}O_d$ changes observed at Wulu and Dongge sites (Fig. 5). If woody vegetation indeed existed in these areas in the distant time (Zhao et al., 2012; Du et al., 2013), persistence of centennial-scale $\delta^{13}C$ variability apparently does not support an interpretation of alternation between C_3 and C_4 plants, which is important for millennial-scale speleothem $\delta^{13}C$ variations (Dorale et al., 1992). In Figure 5, the decrease of soil CO_2 production (increase in the calcite $\delta^{13}C_d$) closely follows the rapid AM decline. This correlation indicates a dominant role of water availability on the calcite speleothem $\delta^{13}C$ signal, even if it is amplified by kinetic effects.

Climatic/environmental implications for speleothem $\delta^{18}O$ and $\delta^{13}C$

At these sites, the amplitude of $\delta^{13}C_d$ variability (more than 0.64‰) is generally twice (about 1.7–2.9 times) that of the $\delta^{18}O_d$ (less than 0.38‰) (Fig. 5), and changes of the $\delta^{13}C_d/\delta^{18}O_d$ ratio are generally constant during MIS 3 and the Holocene (Supplementary Fig. 3). It appears that the relatively higher amplitude of centennial-scale $\delta^{13}C$ variability is independent of site-specific processes and climate boundary conditions. Similarly, larger-magnitude calcite $\delta^{13}C$ variations were previously reported at different time scales (Supplementary Table 1) (Burns et al., 2002; Genty et al., 2003; Baldini et al., 2005; Cruz et al., 2006; Frappier et al., 2007; Hodge et al., 2008; Mattey et al., 2008; Scholz et al., 2012). In Hollow Ridge Cave, Florida, a spatial $\delta^{13}C/\delta^{18}O$ slope of 1.7–1.9 was also observed in the active calcite precipitation (Tremaine et al., 2011). These observations imply that the carbon isotope in the DIC is more sensitive to climate changes, or $\delta^{18}O$ and $\delta^{13}C$ signals should have different modes of geochemical behaviors.

At the carbonate−water interface, an establishment of chemical and isotopic equilibrium is believed to be faster for carbon isotopes (10–100s) than oxygen isotopes (several 10,000s), which is significantly influenced by the buffering effect (Dreybrodt and Scholz, 2011). Hence, a rapid $\delta^{13}C$ response is expected as degassing processes could disproportionately affect $\delta^{13}C$ during calcite precipitation. In Supplementary Fig. 3, the slope of $\delta^{13}C_d/\delta^{18}O_d$ exhibits little variability in MIS 3 and the Holocene (within a range of

±0.0007). This suggests that the relationship between $\delta^{13}C_d$ and $\delta^{18}O_d$ in Figure 5 is unaffected by noises associated with changes in geochemical conditions of infiltration water. Nevertheless, shifts of the rainfall $\delta^{18}O$ composition, believed to be inherited by the speleothems, are often reduced in amplitude by mixing (i.e., reservoir effect) in the karst fracture systems (Fairchild et al., 2006). Thus, it is possible that the initial rainfall $\delta^{18}O$ composition might be dampened in the speleothems. In contrast, shifts of the climate and soil conditions, vegetation density and biological activity possibly all contribute to changes of the calcite $\delta^{13}C$, which include climatic and non-climatic processes, probably resulting in exceptionally prominent $\delta^{13}C$ changes. Another possibility is that the ecosystem processes can further amplify the climatic signals (Frappier et al., 2002).

Moreover, the time scales on which the $\delta^{13}C_d$ and $\delta^{18}O_d$ co-varies are strikingly different in the Holocene (about 150 yr) and the glacial (about 300 yr) (Fig. 6a−d). Dynamically, these centennial periodicities shouldn't arise from site-specific processes. Critically, the effect of kinetic fractionation, which is frequently stochastic and not strictly dependent on climate variability, is unlikely to precisely lock $\delta^{13}C$ and $\delta^{18}O$ variations into a particular rhythm. If this coupling is of climatic origin, it should be of regional significance.

As the NGRP ice-core record, based on annually counted time scale extending back to the last 60 ka (GICC05, Svensson et al., 2008), has been widely accepted as a template for synchronizing regional or hemispheric geologic records (Blunier et al., 2007; Lowe et al., 2008; Rasmussen et al., 2008; Lemieux-Dudon et al., 2010), here the 20-yr-resolved NGRP $\delta^{18}O$ data are applied for comparison. In the Holocene, centennial-scale AM variability was suggested to be closely correlated with changes of the Greenland temperature (Wang et al., 2005), and the Bond events identified in the North Atlantic sediments (Bond et al., 1997) are clearly reflected in the DA and NGRIP $\delta^{18}O$ records (Fig. 7a and b) (Wang et al., 2005; Svensson et al., 2008). When detrended and smoothed, centennial changes in NGRIP $\delta^{18}O_d$ are partly reflected in the DA $\delta^{18}O_d$ and $\delta^{13}C_d$ records (thick lines in Fig. 7c and d). Cross-wavelet analysis between DA $\delta^{13}C_d$ and NGRIP $\delta^{18}O_d$ records reveals a common periodicity of about 150 yr (Fig. 6e). In detail, the $\delta^{13}C_d$ enrichments surrounding 8.2 and 4.2 ka are broadly consistent with the Greenland temperature decline (Fig. 7e and f). During the last 8.8 ka, however, significant discrepancy can be observed between DA and NGRIP records, and the correlation coefficient between them is small (r = −0.02 to −0.03, n = 444) (Fig. 7c and d). This mismatch mainly comes at decadal scales. A weak correlation between decadal changes of DA and GISP2, GRIP $\delta^{18}O$ records was also noticed by Wang et al. (2005), possibly reflecting uncertainties associated with data resolution and dating errors, regional climate responses, modulation of karstic processes and/or other noises unrecognized. Irrespective of spatial disparity in regional rainfall amount within the AM area (Ding et al., 2008), changes in the soil humidity, controlled by the local ratio of precipitation to evaporation, are important for calcite $\delta^{13}C$ signal and should introduce non-negligible site-specific noises. Furthermore, inconsistency among the Holocene Greenland ice core records, which has been pointed out by Johnsen et al. (2001), might to some extent contribute to the difference between DA and NGRIP records.

Similarly, synchroneity of sub-millennial-scale AM and Greenland temperature variations have been reported in early MIS 3 (Fig. 8a and b) (Svensson et al., 2008; Liu et al., 2010). When aligned to the original (Fig. 8a and b) and detrended Wu23 chronology (purple lines in Fig. 8c and d), centennial changes of NGRIP $\delta^{18}O_d$ parallel the Wu23 $\delta^{18}O_d$ (gray line in Fig. 8c) and $\delta^{13}C_d$ records (gray line in Fig. 8d). Between 60 and 55.5 ka, the Greenland temperature decline closely matches the AM depression and decrease of soil CO_2 production, especially in the sub-stages of DO
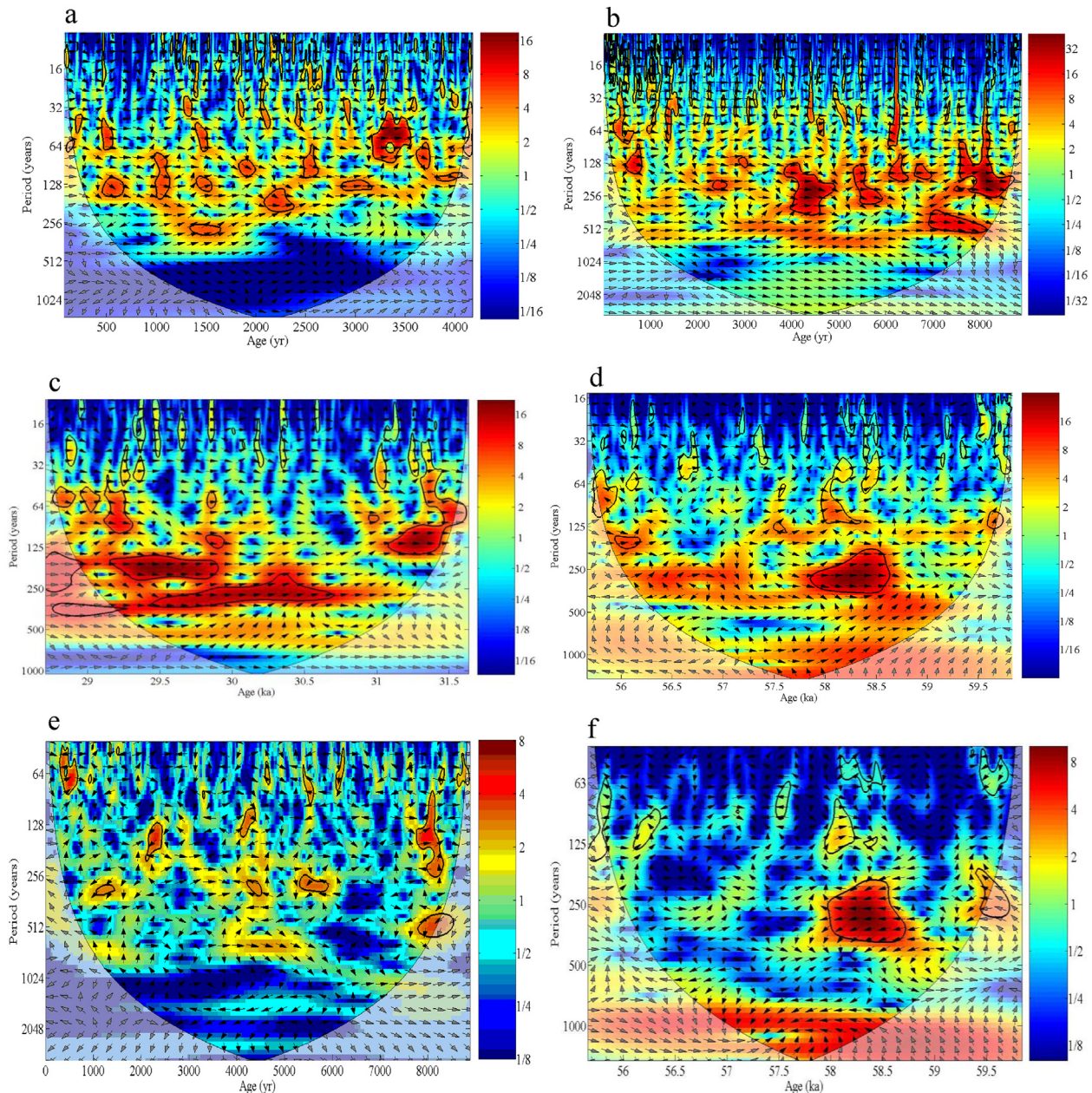
Figure 6. Cross-wavelet analysis between the $\delta^{13}C_d$ and $\delta^{18}O_d$ records for each stalagmite, i.e., samples DAS (a), DA (b), Wu66 (c), Wu23 (d), and (e) DA $\delta^{13}C_d$ and NGRIP $\delta^{18}O_d$, (f) Wu23 $\delta^{13}C_d$ and NGRIP $\delta^{18}O_d$. The spectra were estimated using a method of cross wavelet transform (XWT), yielding common cycles of 150 yr in the Holocene (a and b) and 300 yr in the last glacial period (c and d). Spectral power (variance) is shown by colors ranging from deep blue (weak) to deep red (strong). The 5% significance level against red noise is shown as the thick contour. All data are calculated by the MatLab wavelet coherence package available at http://noc.ac.uk/using-science/crosswavelet-wavelet-coherence. (For interpretation of the references to color in this figure legend, the reader is referred to the web version of this article.)

events (gray bars in Fig. 8c and d). A common cycle of about 300 yr can be identified between Wu23 $\delta^{13}C_d$ and NGRIP $\delta^{18}O_d$ records (Fig. 6f). These observations indicate that at centennial scales the calcite $\delta^{13}C$ can partly reflect climate changes over broad regions, possibly via the soil humidity level. Thus, the low-frequency $\delta^{13}C_d$ cycles (about 300 yr) in early and late MIS 3 (Fig. 6c and d) might be attributed to modulation of glacial background climate conditions, such as those associated with changes of northern summer insolation or continental ice sheets. It is currently beyond our scope to determine to what degree and at what time scales the speleothem $\delta^{13}C$ records can reflect climate changes. However, an important implication for centennial co-variation of $\delta^{13}C$ and $\delta^{18}O$ records we observed at Wulu and Dongge caves is that the speleothem $\delta^{13}C$

signal can contain the information of centennial-scale climate changes, regardless of absence of orbital to millennial variability.

Conclusion

Four high-resolution speleothem $\delta^{13}C$ records from two caves in southern China allow a detailed investigation on the soil/biological processes during early and late MIS 3 and the Holocene. Unlike the $\delta^{18}O$ records, which is strongly influenced by precessional to millennial-scale AM changes, these $\delta^{13}C$ signals exhibit multi-decadal to centennial oscillations around a stable background value. However, at multi-decadal to centennial scales, two isotopic records are closely correlated, and the amplitude of $\delta^{13}C$ variability

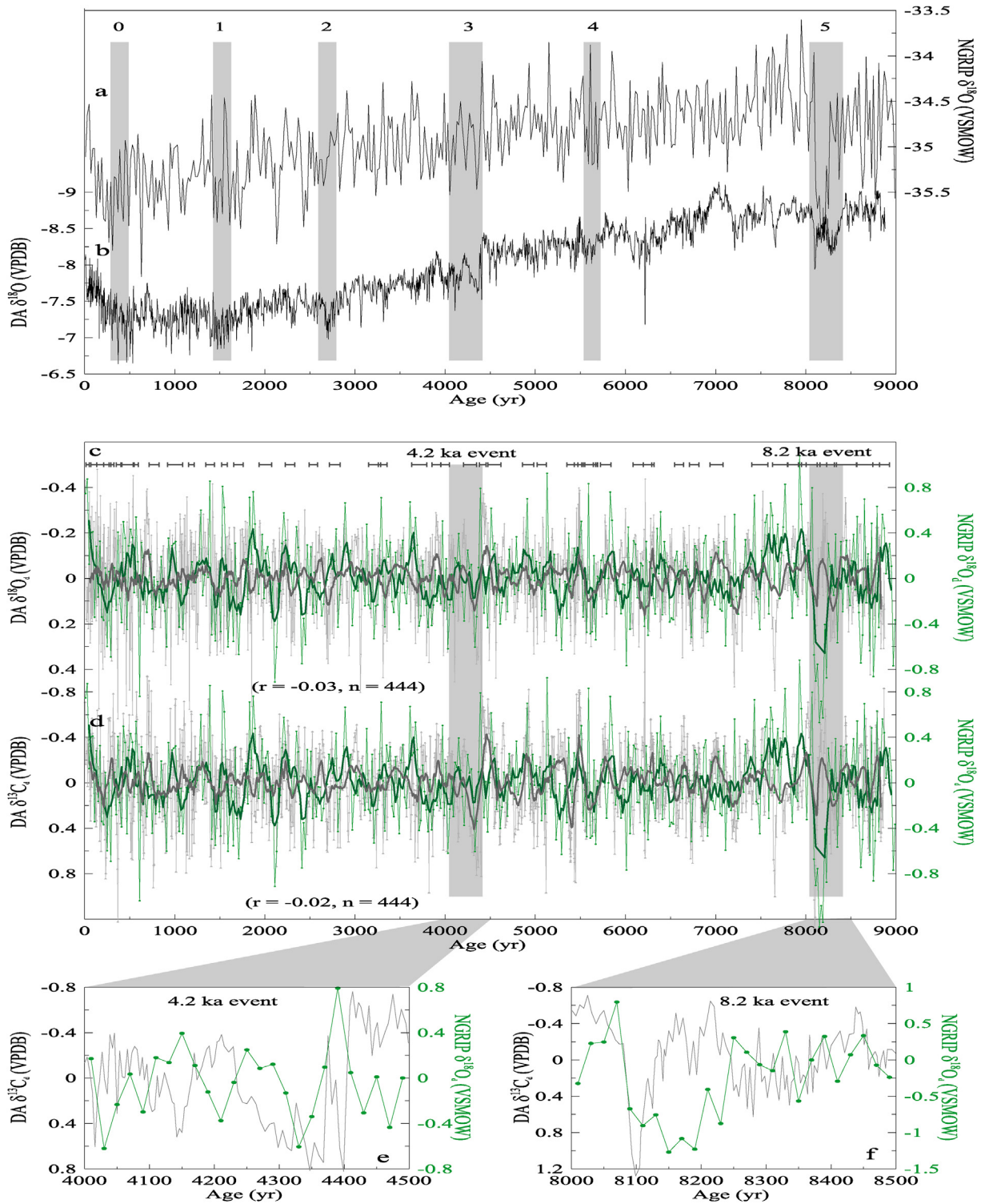**Figure 7.** Correlation of DA $\delta^{18}O$ (Wang et al., 2005), $\delta^{13}C$ and NGRIP ice-core $\delta^{18}O$ records (Svensson et al., 2008). The original $\delta^{18}O$ records from NGRIP (a) and sample DA (b) were drawn in the upper panel. Detrended data of NGRIP $\delta^{18}O$ (c, d, green curve), DA $\delta^{18}O$ (c, gray curve) and DA $\delta^{13}C$ (d, gray curve) are indicated in the middle panel. Error bars for sample DA are depicted at the top of middle panel. Profiles e and f are enlarged plots of DA $\delta^{13}C_d$ and NGRIP $\delta^{18}O_d$ changes surrounding 4.2 and 8.2 ka. The gray bars and the numbers in the upper panel show the Bond events (Bond et al., 1997). In the middle panel, the thicker lines depict the 100-yr running mean, and the correlation coefficients, performed between DA and NGRIP records in the last 8.8 ka, were analyzed with 20-yr linearly interpolated data. (For interpretation of the references to color in this figure legend, the reader is referred to the web version of this article.)

is averagely twice of the $\delta^{18}O$, highlighting a climatic origin of the $\delta^{13}C$ signal, even if it is amplified by kinetic effects.

Cross-spectral analysis between the detrended $\delta^{18}O$ and $\delta^{13}C$ data reveals different coupling cycles in the last glacial period (about 300 yr) and the Holocene (about 150 yr). Regardless of absence of precessional and millennial variability, those centennial-scale $\delta^{13}C$ changes broadly correlate with Greenland temperature variations, implying a common climate response over wide regions.
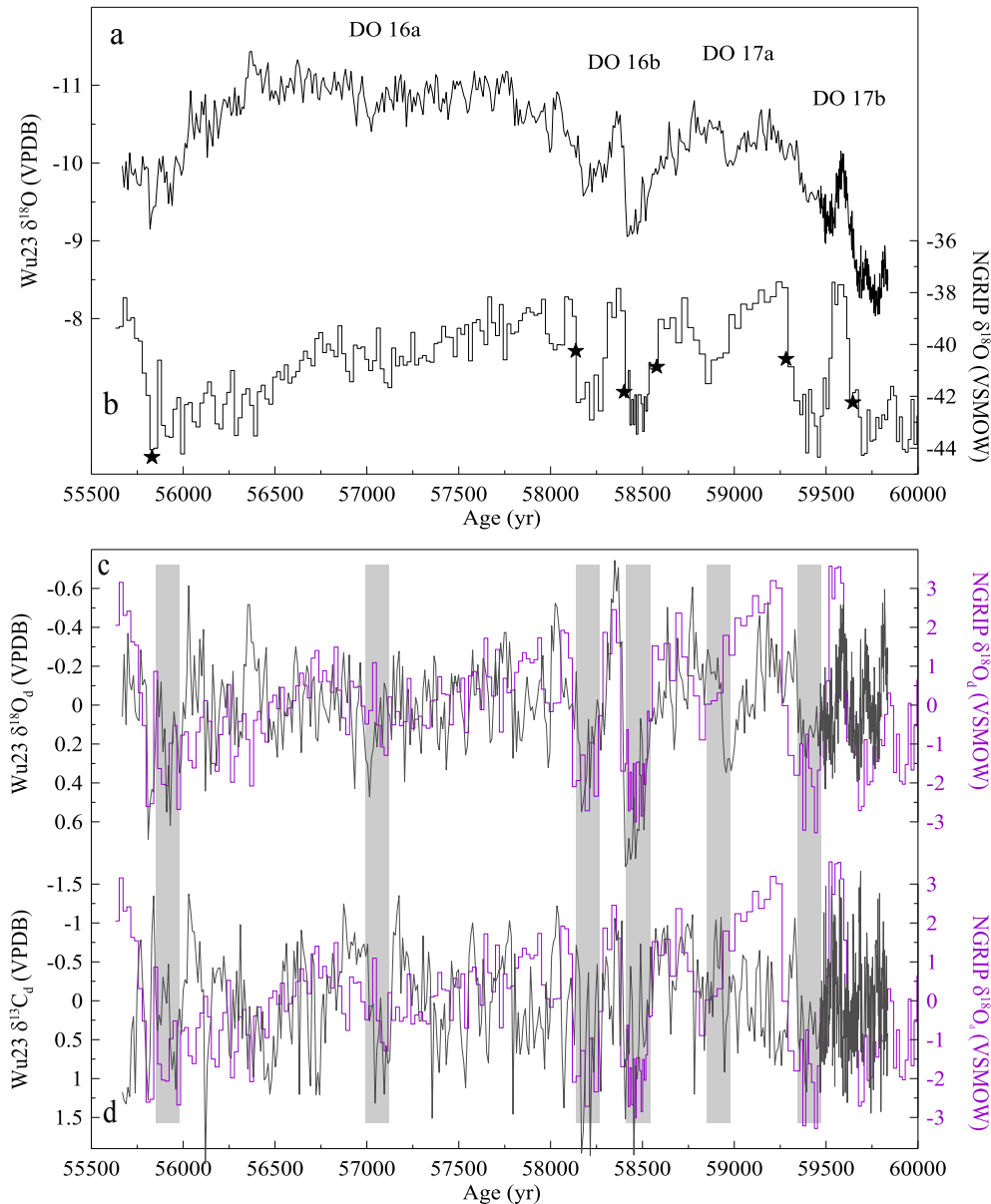
Figure 8. Comparison of NGRIP $\delta^{18}O_d$ record (pink curves in c and d) with Wu23 $\delta^{18}O_d$ (gray curve in c) and $\delta^{13}C_d$ records (gray in d). The NGRIP $\delta^{18}O$ record was first aligned to the Wu23 $\delta^{18}O$ record (a, b). The asterisks in curve b indicate the time points applied here. In the lower panel, the gray bars show concurrent response of NGRIP $\delta^{18}O$, Wu23 $\delta^{18}O$ and $\delta^{13}C$ records in the sub-stages of DO events. (For interpretation of the references to color in this figure legend, the reader is referred to the web version of this article.)

If the observed co-variation of centennial-scale $\delta^{13}C$ and $\delta^{18}O$ changes is further confirmed, the calcite $\delta^{13}C$ signal can be used to promote our understanding of centennial-scale climate changes and as a geochronological marker.

Appendix A. Supplementary data

Supplementary data related to this article can be found at http://dx.doi.org/10.1016/j.yqres.2016.02.008.

References

Arnone III, J.A., Verburg, P.S.J., Johnson, D.W., Larsen, J.D., Jasoni, R.L., Lucchesi, A.J., Batts, C.M., von Nagy, C., Coulombe, W.G., Schorran, D.E., Buck, P.E., Braswell, B.H., Coleman, J.S., Sherry, R.A., Wallace, L.L., Luo, Y.Q., Schimel, D.S., 2008. Prolonged suppression of ecosystem carbon dioxide uptake after an anomalously warm year. Nature 455, 383–386.

Baker, A., Ito, E., Smart, P.L., McEwan, R.F., 1997. Elevated and variable values of ^{13}C in speleothems in a British cave system. Chemical Geology 136, 263–270.

Baldini, J.U.L., McDermott, F., Baker, A., Baldini, L.M., Mattey, D.P., Railsback, L.B., 2005. Biomass effects on stalagmite growth and isotope ratios: a 20th century analogue from Wiltshire, England. Earth and Planetary Science Letters 240, 486–494.

Blunier, T., Spahni, R., Barnola, J.-M., Chappellaz, J., Loulergue, L., Schwander, J., 2007. Synchronization of ice core records via atmospheric gases. Climate of the Past 3, 325–330.

Blyth, A.J., Smith, C.I., Drysdale, R.N., 2013. A new perspective on the δ^{13}C signal preserved in speleothems using LC-IRMS analysis of bulk organic matter and compound specific isotope analysis. Quaternary Science Reviews 75, 143–149.

Bond, G., Showers, W., Cheseby, M., Lotti, R., Almasi, P., deMenocal, P., Priore, P., Cullen, H., Hajdas, I., Bonani, G., 1997. A pervasive millennial-scale cycle in North Atlantic Holocene and glacial climates. Science 278, 1257–1266.

Burns, S.J., Fleitmann, D., Mudelsee, M., Neff, U., Matter, A., Mangini, A., 2002. A 780-year annually resolved record of Indian Ocean monsoon precipitation from a speleothem from south Oman. Journal of Geophysical Research 107 (D20), 4434. http://dx.doi.org/10.1029/2001JD001281.

Burns, S.J., Fleitmann, D., Matter, A., Kramers, J., Al-Subbary, A.A., 2003. Indian ocean climate and an absolute chronology over Dansgaard/Oeschger events 9 to 13. Science 301, 1365–1367.

Cai, Y.J., An, Z.S., Cheng, H., Edwards, R.L., Kelly, M.J., Liu, W.G., Wang, X.F., Shen, C.-C., 2006. High-resolution absolute-dated Indian Monsoon record between 53 and 36 ka from Xiaobailong Cave, southwestern China. Geology 34, 621–624.

Carvalhais, N., Forkel, M., Khomik, M., Bellarby, J., Jung, M., Migliavacca, M., Mu, M.Q., Saatchi, S., Santoro, M., Thurner, M., Weber, U., Ahrens, B., Beer, C., Cescatti, A., Randerson, J.T., Reichstein, M., 2014. Global covariation of carbon turnover times with climate in terrestrial ecosystems. Nature 514, 213–217.

Cerling, T.E., Solomon, D.K., Quade, J., Bowman, J.R., 1991. On the isotopic composition of carbon in soil carbon dioxide. Geochimica et Cosmochimica Acta 55, 3403–3405.

Cheng, H., Sinha, A., Wang, X.F., Cruz, F.W., Edwards, R.L., 2012. The Global Paleomonsoon as seen through speleothem records from Asia and the Americas. Climate Dynamics. http://dx.doi.org/10.1007/s00382-012-1363-7.

Conant, R.T., Ryan, M.G., Ågren, G.I., Birge, H.E., Davidson, E.A., Eliasson, P.E., Evans, S.E., Frey, S.D., Giardina, C.P., Hopkins, F.M., Hyvönen, R., Kirschbaum, M.U.F., Lavallee, J.M., Leifeld, J., Parton, W.J., Steinweg, J.M., Wallenstein, M.D., Wetterstedt, J.Å.M., Bradford, M.A., 2011. Temperature and soil organic matter decomposition rates — synthesis of current knowledge and a way forward. Global Change Biology 17, 3392–3404.

Cruz, J.F.W., Burns, S.J., Karmann, I., Sharp, W.D., Vuille, M., Ferrari, J.A., 2006. A stalagmite record of changes in atmospheric circulation and soil processes in the Brazilian subtropics during the Late Pleistocene. Quaternary Science Reviews 25, 2749–2761.

Deininger, M., Fohlmeister, J., Scholz, D., Mangini, A., 2012. Isotope disequilibrium effects: the influence of evaporation and ventilation effects on the carbon and oxygen isotope comparison of speleothems — a model approach. Geochimica et Cosmochimica Acta 96, 57–79.

Ding, Y.H., Wang, Z.Y., Sun, Y., 2008. Inter-decadal variation of the summer precipitation in East China and its association with decreasing Asian summer monsoon. Part I: observed evidences. International Journal of Climatology 28, 1139–1161.

Dorale, J.A., González, L.A., Reagan, M.K., Pickett, D.A., Murrell, M.T., Baker, R.G., 1992. A high-resolution record of Holocene climate change in speleothem calcite from Cold Water Cave, northeast Iowa. Science 258, 1626–1630.

Dorale, J.A., Liu, Z., 2009. Limitations of Hendy Test criteria in judging the paleoclimatic suitability of speleothems and the need for replication. Journal of Cave and Karst Studies 71, 73–80.

Dreybrodt, W., Scholz, D., 2011. Climatic dependence of stable carbon and oxygen isotope signals recorded in speleothem: from soil water to speleothem calcite. Geochimica et Cosmochimica Acta 75, 734–752.

Dreybrodt, W., Deininger, M., 2014. The impact of evaporation to the isotope composition of DIC in calcite precipitating water films in equilibrium and kinetic fractionation models. Geochimica et Cosmochimica Acta 125, 433–439.

Du, R.R., Chen, J.A., Zeng, Y., Zhu, Z.J., 2013. Climate change recorded mainly by pollen from baiixian lake during the last 5.5 ka B.P. Acta Ecologica Sinica 33, 3783–3791 (in Chinese).

Duan, F.C., Wang, Y.J., Shen, C.-C., Wang, Y., Cheng, H., Wu, C.-C., Hu, H.-M., Kong, X.G., Liu, D.B., Zhao, K., 2014a. Evidence of solar cycles in a late Holocene speleothem record from Dongge Cave, China. Nature Scientific Report 4, 5159. http://dx.doi.org/10.1038/srep05159.

Duan, F.C., Liu, D.B., Cheng, H., Wang, X.F., Wang, Y.J., Kong, X.G., Chen, S.T., 2014b. A high-resolution monsoon record of millennial-scale oscillations during Late MIS 3 from Wulu Cave, south-west China. Journal of Quaternary Science 29, 83–90.

Fairchild, I.J., Smith, C.L., Baker, A., Fuller, L., Spötl, C., Mattey, D., McDermott, F., E.I.M.F, 2006. Modification and preservation of environmental signals in speleothems. Earth-Sciences Reviews 75, 105–153.

Feng, W.M., Casteel, R.C., Banner, J.L., Heinze-Fry, A., 2014. Oxygen isotope variations in rainfall, drip-water and speleothem calcite from a well-ventilated cave in Texas, USA: assessing a new speleothem temperature proxy. Geochimica et Cosmochimica Acta 127, 233–250.

Frappier, A., Sahagian, D., González, L.A., Carpenter, S.J., 2002. El Niño events recorded by stalagmite carbon isotopes. Science 298, 565.

Frappier, A.B., Sahagian, D., Carpenter, S.J., González, L.A., Frappier, B.R., 2007. Stalagmite stable isotope record of recent tropical cyclone events. Geology 35, 111–114.

Genty, D., Baker, A., Massault, M., Proctor, C., Gilmour, M., Pons-Branchu, E., Hamelin, B., 2001. Dead carbon in stalagmites: carbonate bedrock paleo-dissolution vs. ageing of soil organic matter. Implications for ^{13}C variations in speleothems. Geochimica et Cosmochimica Acta 65, 3443–3457.

Genty, D., Blamart, D., Ouahdi, R., Gilmour, M., Baker, A., Jouzel, J., Van-Exter, S., 2003. Precise dating of Dansgaard-Oeschger climate oscillations in western Europe from stalagmite data. Nature 421, 833–837.

Genty, D., Blamart, D., Ghaleb, B., Plagnes, V., Causse, Ch., Bakalowicz, M., Zouari, K., Chkir, N., Hellstrom, J., Wainer, K., Bourges, F., 2006. Timing and dynamics of the last deglaciation from European and North African δ^{13}C stalagmite profiles—comparison with Chinese and South Hemisphere stalagmites. Quaternary Science Reviews 25, 2118–2142.

Grünzweig, J.M., Hemming, D., Maseyk, K., Lin, T.B., Rotenberg, E., Raz-Yaseef, N., Falloon, P.D., Yakir, D., 2009. Water limitation to soil CO_2 efflux in a pine forest at the semiarid "timberline". Journal of Geophysical Research 114, G03008. http://dx.doi.org/10.1029/2008JG000874.

Hellstrom, J., McCulloch, M., Stone, J., 1998. A detailed 31,000-year record of climate and vegetation change, from the isotope geochemistry of two New Zealand speleothems. Quaternary Research 50, 167–178.

Hendy, C.H., 1971. The isotopic geochemistry of speleothems-I. The calculation of the effects of different modes of formation on the isotopic composition of speleothems and their applicability as paleoclimatic indicators. Geochimica et Cosmochimica Acta 35, 801–824.

Hercman, H., Pawlak, J., 2012. MOD-AGE: an age-depth model construction algorithm. Quaternary Geochronology 12, 1–10.

Hodge, E.J., Richard, D.A., Smart, P.L., Andreo, B., Hoffmann, D.L., Mattey, D.P., González-Ramón, A., 2008. Effective precipitation in south Spain (~ 266 to 46 ka) based on a speleothem stable carbon isotope record. Quaternary Research 69, 447–457.

Jiang, Z.C., Lian, Y.Q., Qin, X.Q., 2014. Rocky desertification in Southwest China: impacts, cause, and restoration. Earth-Science Reviews 132, 1–12.

Johnsen, S.J., Dahl-Jensen, D., Gundestrup, N., Steffensen, J.P., Clausen, H.B., Miller, H., Masson-Delmotte, V., Sveinbjörnsdottir, A.E., White, J., 2001. Oxygen isotope and palaeotemperature records from six Greenland ice-core stations: Camp Century, Dye-3, GRIP, GISP2, Renland and NorthGRIP. Journal of Quaternary Science 16, 299–307.

Johnston, V.E., Borsato, A., Spötl, C., Frisia, S., Miotandi, R., 2013. Stable isotopes in caves over altitudinal gradients: fractionation behaviour and inferences for speleothem sensitivity to climate change. Climate of the Past 9, 99–118.

Keeling, C.D., Mook, W.G., Jans, P.P., 1979. Recent trend in the ^{13}C/^{12}C ratio of atmospheric carbon dioxide. Nature 277, 121–123.

Kirschbaum, M.U.F., 1995. The temperature dependence of soil organic matter decomposition, and the effect of global warming on soil organic C storage. Soil Biology & Biochemistry 27, 753–760.

Kong, X.G., Wang, Y.J., Wu, J.Y., Cheng, H., Edwards, R.L., Wang, X.F., 2005. Complicated response of stalagmite δ^{13}C to climate change during the last glaciation from Hulu Cave, Nanjing, China. Science in China Series D: Earth Sciences 48, 2174–2181.

Lambert, W.J., Aharon, P., 2011. Controls on dissolved inorganic carbon and δ^{13}C in a cave waters from DeSoto Caverns: implications for speleothem δ^{13}C assessments. Geochimica et Cosmochimica Acta 75, 753–768.

Lemieux-Dudon, B., Blayo, E., Petit, J.-R., Waelbroeck, C., Svensson, A., Ritz, C., Barnola, J.-M., Narcisi, B.M., Parrenin, F., 2010. Consistent dating of Antarctic and Greenland ice cores. Quaternary Science Reviews 29, 8–20.

Liu, D.B., Wang, Y.J., Cheng, H., Edwards, R.L., Kong, X.G., Wang, X.F., Hardt, B., Wu, J.Y., Chen, S.T., Jiang, X.Y., He, Y.Q., Dong, J.G., Zhao, K., 2010. Sub-millennial variability of Asian monsoon intensity during the early MIS 3 and its analogue to the ice age terminations. Quaternary Science Reviews 29, 1107–1115.

Lowe, J.J., Rasmussen, S.O., Björck, S., Hoek, W.Z., Steffensen, J.P., Walker, M.J.C., Yu, Z.C., the INTIMATE group, 2008. Synchronisation of palaeoenvironmental events in the North Atlantic region during the Last Termination: a revised protocol recommended by the INTIMATE group. Quaternary Science Reviews 27, 6–17.

Mattey, D., Lowry, D., Duffet, J., Fisher, R., Hodge, E., Frisia, S., 2008. A 53 year seasonally resolved oxygen and carbon isotope record from a modern Gibraltar speleothem: reconstructed drip water and relationship to local precipitation. Earth and Planetary Science Letters 269, 80–95.

McDermott, F., 2004. Palaeo-climate reconstruction from stable isotope variations in speleothems: a review. Quaternary Science Reviews 23, 901–918.

Meyer, K.W., Feng, W.M., Breecker, D.O., Banner, J.L., Guilfoyle, A., 2014. Interpretation of speleothem calcite δ^{13}C variations: evidence from monitoring soil CO_2, drip water, and modern speleothem calcite in central Texas. Geochimica et Cosmochimica Acta 142, 281–298.

Mickler, P.J., Banner, J.L., Stern, L., Asmerom, Y., Edwards, R.L., Ito, E., 2004. Stable isotope variations in modern tropical speleothems: evaluating equilibrium vs. kinetic isotope effects. Geochimica et Cosmochimica Acta 68, 4381–4393.

Mickler, P.J., Stern, L.A., Banner, J.L., 2006. Large kinetic isotope effects in modern speleothems. Geological Society of America Bulletin 118, 65–81.

Mühlinghaus, C., Scholz, D., Mangini, A., 2007. Modelling stalagmite growth and δ^{13}C as a function of drip interval and temperature. Geochimica et Cosmochimica Acta 71, 2780–2790.

Mühlinghaus, C., Scholz, D., Mangini, A., 2009. Modelling fractionation of stable isotopes in stalagmites. Geochimica et Cosmochimica Acta 73, 7275–7289.

Rasmussen, S.O., Seierstad, I.K., Andersen, K.K., Bigler, M., Dahl-Jensen, D., Johnsen, S.J., 2008. Synchronization of the NGRIP, GRIP, and GISP2 ice cores

across MIS 2 and paleoclimatic implications. Quaternary Science Reviews 27, 18–28.

Ridley, H.E., Asmerom, Y., Baldini, J.U.L., Breitenbach, S.F.M., Aquino, V.V., Prufer, K.M., Culleton, B.J., Polyak, V., Lechleitner, F.A., Kennett, D.J., Zhang, M.H., Marwan, N., Macpherson, C.G., Baldini, L.M., Xiao, T.Y., Peterkin, J.L., Awe, J., Haug, G.H., 2015. Aerosol forcing of the position of the intertropical convergence zone since AD 1550. Nature Geoscience 8, 195–200.

Romanov, D., Kaufmann, G., Dreybrodt, W., 2008. δ^{13}C profiles along growth layers of stalagmites: comparing theoretical and experimental results. Geochimica et Cosmochimica Acta 72, 438–448.

Scholz, D., Mühlinghaus, C., Mangini, A., 2009. Modelling δ^{13}C and δ^{18}O in the solution layer on stalagmite surfaces. Geochimica et Cosmochimica Acta 73, 2592–2602.

Scholz, D., Frisia, S., Borsato, A., Spötl, C., Fohlmeister, J., Mudelsee, M., Miorandi, R., Mangini, A., 2012. Holocene climate variability in north-eastern Italy: potential influence of the NAO and solar activity recorded by speleothem data. Climate of the Past 8, 1367–1383.

Shen, C.-C., Edwards, R.L., Cheng, H., Dorale, J.A., Thomas, R.B., Moran, S.B., Weinstein, S.E., Edmonds, H.N., 2002. Uranium and thorium isotopic and concentration measurements by magnetic sector inductively coupled plasma mass spectrometry. Chemical Geology 185, 165–178.

Stoll, H., Mendez-Vicente, A., Gonzalez-Lemos, S., Moreno, A., Cacho, I., Cheng, H., Edwards, R.L., 2015. Interpretation of orbital scale variability in mid-latitude

speleothem δ^{18}O: significance of growth rate controlled kinetic fractionation effects. Quaternary Science Reviews 127, 215–228.

Svensson, A., Andersen, K.K., Bigler, M., Clausen, H.B., Dahl-Jensen, D., Davies, S.M., Johnsen, S.J., Muscheler, R., Parrenin, F., Rasmussen, S.O., Röthlisberger, R., Seierstad, I., Steffensen, J.P., Vinther, B.M., 2008. A 60 000 year Greenland stratigraphic ice core chronology. Climate of the Past 4, 47–57.

Tremaine, D.M., Froelich, P.N., Wang, Y., 2011. Speleothem calcite farmed in situ: modern calibration of δ^{18}O and δ^{13}C paleoclimate proxies in a continuously-monitored natural cave system. Geochimica et Cosmochimica Acta 75, 4929–4950.

Trumbore, S.E., 1997. Potential responses of soil organic carbon to global environmental change. Proceedings of the National Academy of Sciences of the United States of America 94, 8284–8291.

Wang, Y.J., Cheng, H., Edwards, R.L., He, Y.Q., Kong, X.G., An, Z.S., Wu, J.Y., Kelly, M.J., Dykoski, C.A., Li, X.D., 2005. The Holocene Asian monsoon: links to solar changes and North Atlantic climate. Science 308, 854–857.

Zhao, K., Wang, Y.J., Edwards, R.L., Cheng, H., Liu, D.B., 2010. High-resolution stalagmite δ^{18}O records of Asian monsoon changes in central and southern China spanning the MIS 3/2 transition. Earth and Planetary Science Letters 298, 191–198.

Zhao, Z.Y., Yuan, D.X., Shi, S.Q., Luo, L.D., 2012. MIS3b vegetation and climate changes based on pollen and charcoal on Qianxi Plateau. Acta Ecologica Sinica 32, 4811–4818 (in Chinese).